JOURNAL OF GEOPHYSICAL RESEARCH, VOL. 97, NO. B4, PAGES 5145–5151, APRIL 10, 1992

Permeability of Core Samples From Cajon Pass Scientific Drill Hole: Results From 2100 to 3500 m Depth

C. A. MORROW AND J. D. BYERLEE

U.S. Geological Survey, Menlo Park, California

Hydrologic rock properties are important to the debate about the state of stress and heat flow regime of the San Andreas fault. In particular, these properties are pertinent to whether frictional heat generated by high shear stresses can be convected away by circulating ground water, thus accounting for the absence of a measurable heat flow anomaly across the fault. To help resolve this debate, we have conducted laboratory permeability measurements on intact core samples from the Cajon Pass drill hole extracted from depths between 2100 and 3500 m. These rocks were all crystalline in nature, including granodiorites, tonalites, monzogranites and gneisses. Confining and pore pressures matched the in situ pressures for each depth, and distilled water was used as the permeating medium. Permeabilities ranged from 10^{-22} to 10^{-19} m^2 for effective pressures between 36 and 56 MPa. In general, the permeability values decreased with depth in a manner consistent with earlier studies of rocks between 500 and 2100 m in the drill hole. Petrographic observations indicate that repeated episodes of crack healing and sealing are the mechanisms responsible for the extremely low permeability values. Secondary minerals that seal the microfractures include abundant laumontite, calcite, quartz, chlorite, and other phyllosilicates. The permeability results suggest that water circulation in the vicinity of the drill hole must be restricted to major fracture zones, with minimal exchange of water in more intact regions. This finding is consistent with geochemical evidence of little mixing of the pore waters sampled from different sections of the borehole. The results also suggest that massive water circulation through the bulk of the rock is unlikely as a mechanism for obscuring the heat flow anomaly that would be expected if shear stresses along the San Andreas fault are high.

INTRODUCTION

The state of stress on the San Andreas fault has long been a subject of debate. Frictional faulting theory and laboratory strength data of rocks and fault gouges suggest that shear stresses along the fault are high, of the order several tens of megapascals [*Brace and Kohlstedt*, 1980]. This is inconsistent with the evidence from conductive heat flow measurements made in over 100 shallow boreholes near the San Andreas fault. These measurements show no evidence of frictionally generated heat, implying a lower average shear stress of 10–20 MPa [*Lachenbruch and Sass*, 1980]. Such low average shear stresses are consistent with the observed seismic stress drops of earthquakes [*Hanks*, 1977]. One of the theories to explain such a paradox is that the frictionally generated heat may be convected away from the fault by circulating groundwater. This would obscure the expected heat flow anomaly while still satisfying the constraints of laboratory frictional studies.

O'Neil and Hanks [1980] argue that the stable isotope signatures of rocks near the San Andreas have been altered by interaction with groundwater while the rocks were buried deeper in the crust, whereas rocks that are farther away have not been so affected. This would imply that meteoric waters have circulated to great depths in the crust near fault zones, consistent with the theory of convective heat transport. It also implies that fluid pressures were hydrostatic, and therefore the low shear stresses are not the result of overpressured fluids. However, *Lachenbruch and Sass* [1980] argue that the lack of substantial thermal discharge from springs near the fault and the different hydrologic regimes on either side do not support the notion of convective heat dissipation through groundwater circulation. In addition, low-permeability fault gouge material from other faults near the San Andreas vicinity could act as a barrier to lateral fluid flow [*Morrow and Byerlee*, 1988]. Such low permeabilities do not rule out the possibility that overpressured fluids can be generated within the gouge of the San Andreas itself. However, high fluid pressures can not adequately explain the low shear stresses inferred along the San Andreas because the maximum horizontal compression has been found to be nearly normal to the fault [*Zoback et al.*, 1987]. In such a case the high fluid pressures would cause hydrofracturing of the rocks before the reduction in effective stress was sufficient to cause slip on the fault. Clearly, the hydrologic properties of fault zones are important to an understanding of the stress and heat flow environment of the fault.

The Deep Observation and Sampling of the Earth's Continental Crust, Inc. (DOSECC) drill hole at Cajon Pass was intended to resolve some of these long-standing controversies. As part of this program, permeability studies were conducted on cores extracted from the drill hole. This paper presents the permeability results of rocks from 2100 to 3500 m and is a continuation of the work described by *Morrow and Byerlee* [1988]. In these permeability studies, we hope to shed some light on the question of whether frictionally generated heat can be dissipated by massive ground water circulation.

Paper number 90JB00423.

SAMPLE DESCRIPTION

The samples used in this study were recovered from segments between 2100 and 3500 m in the Cajon Pass drill hole, corresponding to the second phase of the drilling program. The specimens are crystalline in nature with a wide range of compositions including granodiorites, tonalites, monzogranites, and gneisses (see Table 1). Rocks from the

TABLE 1. Experimental Results From 2100 to 3500 m

Core	Depth, m	Direction,*	Rock Type	P_c, MPa	P_p, MPa	P_e, MPa	k, 10^{-21} m^2
35/2	2183.2	V	hornblende monzodiorite	57.6	21.4	36.2	4.3
36/5	2247.1	0	hornblende	59.3	22.0	37.3	18.3
		90	biotite tonalite gneiss				6.4
37/3	2287.9	V	granodiorite	60.4	22.4	38.0	8.1
		90	gneiss				4.5
38/2	2350.9	90	gneissic biotite monzogranite	61.9	23.1	38.8	13.2
39/7	2426.0	V	hornblende	64.0	23.8	40.2	1.1
		0	tonalite				217.0
42/1	2604.0	V	biotite	68.7	25.5	43.2	37.2
		0	monzogranite				120.6
		90	gneiss				64.1
44/1	2634.7	V	biotite	69.5	25.8	43.7	185.2
		0	monzogranite gneiss				151.8
45/5	2679.2	V	biotite	70.7	26.3	44.4	0.2
		0	hornblende				0.3
		90	tonalite				0.6
46/7	2742.2	V	biotite	72.3	26.9	45.4	0.8
		0	hornblende				0.7
		90	tonolite gneiss				1.0
48/3	2852.7	0	biotite	75.3	28.0	47.3	0.5
		90	tonalite				1.0
49/1	2887.8	V	granite	76.2	28.3	47.9	0.6
		0	gneiss				0.2
		90					1.2
50/2	3018.9	V	biotite hornblende granodiorite	79.7	29.6	50.1	0.3
51/2	3184.8	V	biotite granodiorite gneiss	84.0	31.2	52.8	271.0
53/2	3404.5	V	biotite	89.8	33.4	56.4	17.9
		90	granodiorite gneiss				7.7

*V, vertical.

second phase of drilling are very heterogeneous on all scales, unlike the homogeneous plutonic units encountered in the shallower sections of the drill hole [*Silver et al.*, 1989]. Fractures containing secondary minerals, such as calcite and laumontite, are common. Care was taken to chose samples from the most unfractured regions of the rock, so as to determine a lower boundary on the permeability of the samples. However, it was not always possible to avoid microfractures; hence not all samples are entirely crack-free. Since such fractures can be identified in thin section, we can compare the permeabilities of these samples with the more unfractured specimens. At each depth chosen for study, the rock was cored in three orthogonal directions as shown in Figure 1 to test for permeability anisotropy. The three cores were labeled V (vertical), 0° (horizontal core drilled at the reference azimuth line), and 90° (horizontal core drilled perpendicular to the reference azimuth line). Some orientations could not be sampled due to the presence of throughgoing fractures. The reference azimuth line was scribed along the length of the cores at the time of retrieval. The true direction of this line relative to north varies widely between the different cores. By comparing downhole electrical images with features observed on the recovered cores, the orientation of many samples from the first phase of drilling was possible [*Pezard and Luthi*, 1988]. This core orientation technique was unsuccessful in the second phase, and therefore the cores used in this study are unoriented.

PROCEDURE

The procedure for measuring the permeability of the core samples between 2100 and 3500 m was the same as that described by *Morrow and Byerlee* [1988] for the shallower

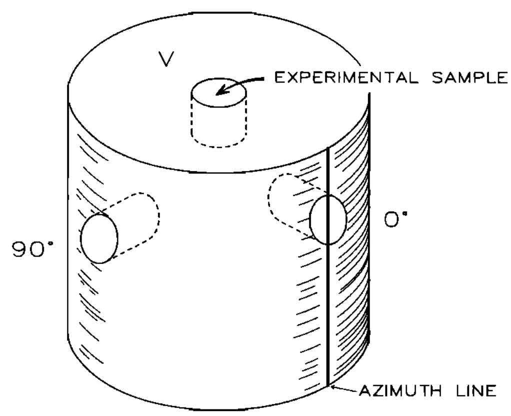

Fig. 1. Orientation of test cores for permeability measurements.

samples. In brief, the core samples were machined into 2.54-cm-diameter cylinders, 2.54 cm long and placed in the experimental assembly as shown in Figure 2. Stainless steel gauze shims on either side of the rock ensured an even distribution of fluid through the sample. The sample column was jacketed with polyurethane to isolate the pore fluid (distilled water) from the confining medium (petroleum ether). Confining pressure was maintained by a computer-controlled servomechanism at the in situ pressure corresponding to the depth of burial for each sample. These overburden pressure values were calculated using an average rock density of 2.69 g/cm^3 determined from the 28 samples tested. Pore pressure was held at the appropriate in situ value assuming a normal hydrostatic gradient by a large reservoir at the outlet side of the sample. The pore pressure inlet was maintained at 1.0 MPa higher than the outlet reservoir by a computer-controlled pressure intensifier. In this way, a steady state flow measurement could be obtained by measuring the change in the volume of the pressure intensifier with time. Very low flow rates can be measured with this system because of the small volume (0.211 mL) of the intensifier reservoir. Temperature was controlled in the experimental chamber at 27° ± 0.5°C to ensure the accuracy of the volume measurements, which are highly sensitive to temperature changes. Flow measurements extended over periods of 1–2 days until a reliable steady state flow was established.

Permeability was determined using Darcy's law:

$$\frac{q}{A}=\frac{k}{\mu}\left(\frac{dP}{dl}\right)$$

where q is the measured flow rate, A is the cross-sectional area of the sample, k is permeability, μ is the dynamic viscosity of water (1.0 cP in these experiments) and dP/dl is the pressure gradient across the length of the sample. Several experiments were conducted at differential pore pressures of 0.5 and 2.0 MPa to compare the 1.0 MPa results. These tests verify that the flow rate is proportional to the pressure drop (double the pressure causes double the flow); therefore Darcy's law holds even for the tightest rocks.

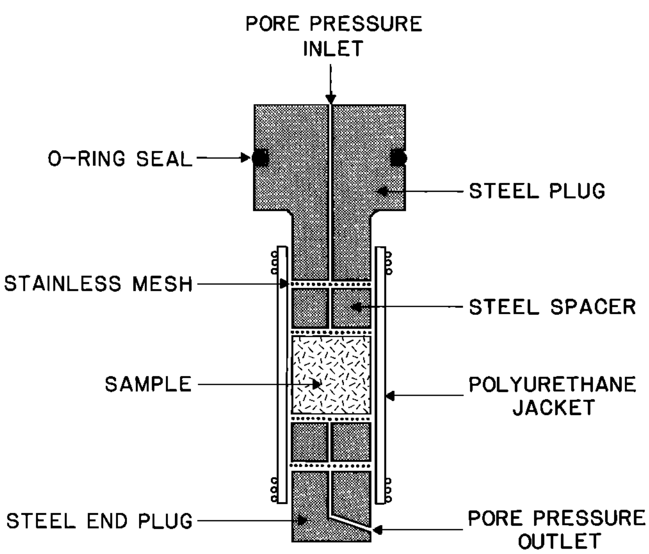

Fig. 2. Sample assembly for steady state flow measurements.

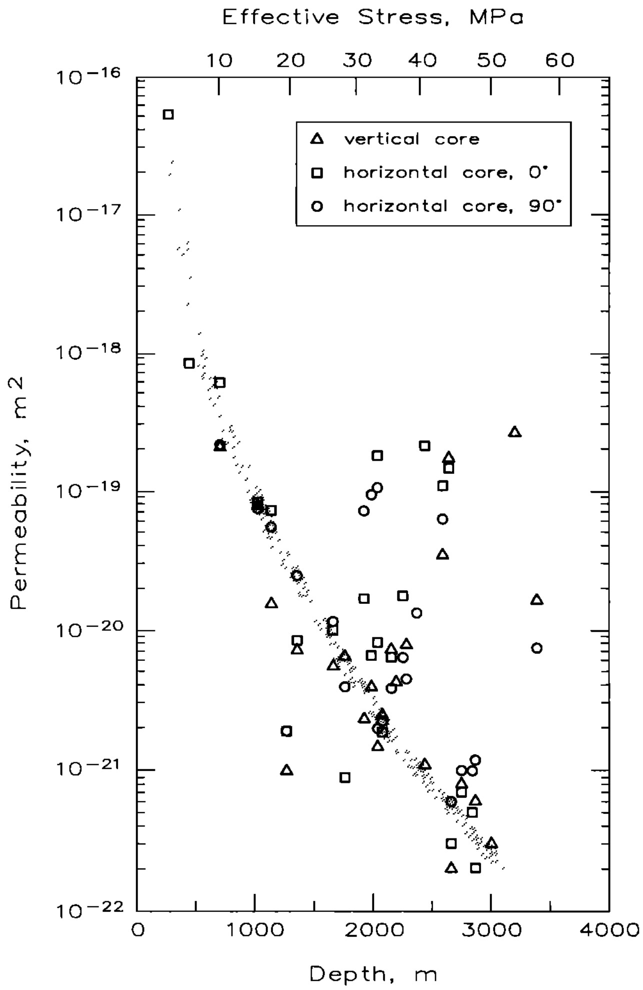

Fig. 3. Permeability of Cajon Pass rocks as a function of depth and effective pressure ($P_c - P_p$). Data <2100 m from *Morrow and Byerlee* [1988]. 10^{-21} m^2 ≃ 1 ndarcy. Data points that fall well above the trend line contain visible fractures that enhance the permeability.

Permeability measurements were accurate to $\pm 2 \times 10^{-22}$m^2 with this experimental system.

PERMEABILITY RESULTS

Permeability values for the 28 samples segments are given in Table 1. Permeability is reported in square meters (1 darcy = 0.987×10^{-12} m^2). Also shown are data on drill core number and segment, depth, orientation relative to azimuth line, lithology, and confining, pore, and effective pressures corresponding to each depth. Permeabilities were generally quite low, ranging between about 10^{-22} to 10^{-19} m^2 for effective pressures of 36–56 MPa. Because the rocks were all tested at different effective pressures, values from Table 1 cannot be compared directly. However, plotted as a function of depth (Figure 3), we can see relative differences between the samples. This plot also contains data from the first phase of drilling (0–2100 m depth) discussed by *Morrow and Byerlee* [1988]. Several points are apparent from Figure 3. First, there is quite a bit of scatter in the data. This scatter is not caused by problems of reproducibility, as numerous tests were repeated which yield the same results. Some samples have permeability values that are significantly higher than other rocks from the same depth (e.g., core 39/7). In other cases, the permeabilities of rocks from nearby depths are quite different, even if we take into account the differences in effective pressure (compare core 44/1 and 45/5 for instance). These variations and their causes are important to the overall interpretation of permeability and will be discussed below. In spite of the large scatter, a majority of the samples appear to follow a decreasing trend of permeability with depth that was more clearly observed with the shallower samples [*Morrow and Byerlee*, 1988]. This rough trend is shown by the curve marked in Figure 3, although it is by no means meant to uniquely characterize the permeability behavior. Permeability decreased by over 1 order of magnitude for every 1000 m in depth. This decrease would be expected due to microcrack closure at the progressively higher effective pressures. Samples that follow this rough trend contained no discernible open fractures in hand specimen or thin section that would tend to increase permeability and therefore probably represent the "intact" permeability of the rocks.

Samples that plot above the trend line in Figure 3 were found to contain fractures that accounted for the higher permeability. Some samples contained cracks clearly visible in hand specimen that appeared as a series of clean, unfilled parallel lines that extended across many grains, or the entire sample. These types of cracks have been interpreted as stress relief fractures that were formed as the rocks were retrieved from depth to atmospheric pressure [*Sun and Wang*, 1989]. Such fractures become more numerous as the drill hole deepens, where overburden pressures are greater. These fractures influence the permeability results due to the fact that the rocks were originally under triaxial stress in the earth, but are placed under a hydrostatic load equal to the overburden pressure in the laboratory. The difference between the laboratory and in situ state of stress may result in incomplete closure of the newly formed cracks. These variations may be small but are important when the bulk permeability is quite low, as is the case with the Cajon Pass samples. Perturbations in the stress profile with depth, as observed by *Zoback and Healy* [1989], may also contribute to differences in the laboratory and in situ stress state. The data in Figure 3 show a sudden onset of scatter at around 1800 m, which is inconsistent with the idea of a gradual increase in fracture density with depth. One possible explanation may be that the tensile strength of the rock must be overcome before fractures can propagate. *Healy and Zoback* [1988] estimate the tensile strength of the rocks to be around 26.5 MPa, based on hydrofracture data. This is slightly below the effective pressure at which we observe the onset of the higher permeability data. It is not clear why some of the deeper samples show visible evidence of stress relief cracking while others do not; however, it is possible that all the rocks are affected by this phenomena to some extent. In this case, the true permeability values would be even lower than those reported here.

Other rocks contained irregular fractures partially or completely filled with secondary minerals that are described in more detail in the following section. Such features were formed in the past and are unrelated to drilling. Many of these natural fractures are throughgoing, and clearly account for some of the higher-permeability data. These different fractures types enhance the permeability of the rocks by up to 2–3 orders of magnitude, as seem in Figure 3. We have not attempted to distinguish cracked or uncracked samples in Figure 3, as there are obviously degrees of fracturing as well as possible combinations of natural and stress relief fractures in any given sample.

Permeabilities were measured in three orthogonal directions to observe the effects of anisotropy in the rocks (notice the vertical spread in the three symbols of Figure 3). With the obvious exception of the samples at 2426 m, differences in the values range up to a factor of about 3. This observed anisotropy may be a result of several factors, including the presence of fractures as discussed above, and variations in the foliation and folding of the rocks. A comparison of permeability and lithology reveals that mineral assemblage does not have much effect on the permeability values, as there was no noticeable difference between the more mafic and sodic samples. In addition, there was no consistent orientation that was more or less permeable than another, when comparing the relative permeabilities at different depths.

Sun and Wang [1989] showed that the fracture directions in oriented cores were related to the regional stress field. Such fracture alignment may contribute to permeability anisotropy in the horizontal direction. Because the 0° and 90° samples in the present study were not oriented relative to north, we would be unable to detect any systematic permeability differences in these directions due to an imposed horizontal stress field. Our main conclusion from the anisotropy tests is that differences in the permeability values do occur between the three orthogonal directions, but they are not significant enough to completely obscure the trend of decreasing permeability with depth.

PETROGRAPHIC OBSERVATIONS

Petrographic studies were conducted on the core samples to determine the cause of the extremely low permeability values, as well as to investigate the properties of natural and induced fractures that may greatly affect the permeability. We have identified three permeability-reducing processes that have been active in the Cajon Pass rocks. These are recrystallization, crack healing, and crack sealing, described below.

Most of the rocks displayed various degrees of recrystallization that reflect several episodes of metamorphic and deformational events [*Silver et al.*, 1989; *Silver and James*, 1989]. One of the more conspicuous recrystallization features relevant to the discussion of fluid flow is the breakdown of minerals, particularly quartz, into a fine-grained fabric with highly tortuous grain boundaries. Figure 4 shows an example of a single quartz grain which is partially recrystallizing in this way. Because permeability is inversely related to crack tortuosity through the Kozeny-Carman equation [*Bear*, 1972], this grain size reduction tends to reduce the permeability by making the flow paths more convoluted through the rock.

Crack healing is another permeability-reducing mechanism that is clearly evident in these samples. Healed cracks are filled with the same mineral as the host grain, in crystalographic and optical continuity. Figure 5 shows several strings of fluid inclusions in a recrystallizing quartz grain that mark the remains of preexisting cracks. We can no longer see the crack boundaries in the grain because of the continuity of the filling and host quartz. This example

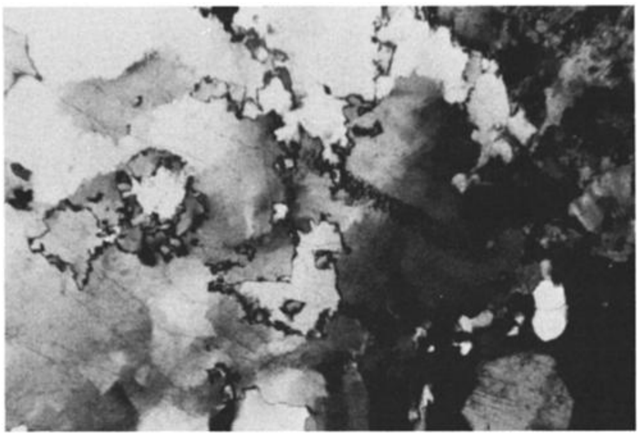

Fig. 4. Quartz grain in a granite gneiss at 2887 m (k = 6.0 × 10^{-22} m^2). The quartz is partially recrystallized into smaller grains with convoluted grain boundaries. 3.6-mm-wide image.

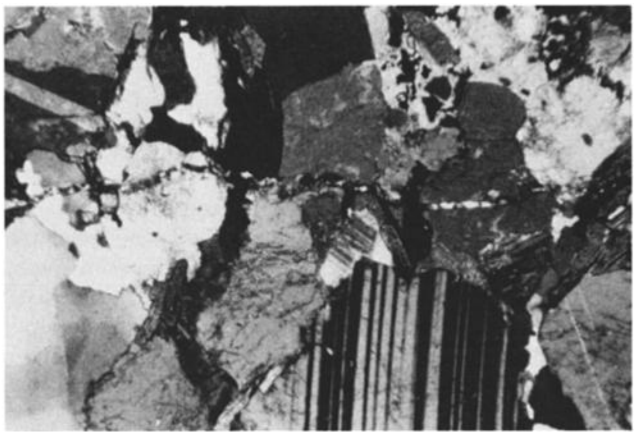

Fig. 6. Laumontite filled fracture cuts horizontally across a biotite hornblende tonalite gneiss at 2742 m. 3.6-mm-wide image.

illustrates that crack healing need not be complete to greatly affect the permeability of the rock, because flow is completely inhibited as soon as the fluid pockets become isolated with no interconnecting network. In the Cajon Pass rocks, such cracks appear to be an older feature, as there are other alteration and/or deformation fabrics that overprint the healed grains. These observations are consistent with the findings of *Sun and Wang* [1989].

Crack sealing is also readily observed in petrographic sections of the Cajon Pass samples. A sealed crack by definition can be filled with any secondary mineral(s), with no crystallographic continuity between the sealing material and the host grain. Secondary minerals in these samples include laumontite, calcite, feldspar and quartz, chlorite, and other phyllosilicates. Laumontite is particularly abundant and is thought to be depositing at the present time (*E. James*, personal communication, 1989). The sealed cracks tend to extend over a much larger area than the healed cracks previously described. In some cases they cut across the entire petrographic thin section. This is a small-scale manifestation of the mineralized fractures of many centimeters in thickness that were observed in the drill core. Such cracks are important for permeability studies, as they influence fluid flow over a broad area. Figure 6 shows a laumontite filled fracture that cuts through the grains of a biotite hornblende tonalite gneiss at 2742 m depth. This rock has a permeability of only 1 × 10^{-21} m^2, due to the fact that the laumontite completely fills the fracture, leaving no major path for fluid flow. In other cases, partially filled fractures have left open pathways, which have the opposite effect on permeability. We observed many examples where the walls of filled fractures were thinly lined with phyllosilicates such as chlorite or biotite which were introduced in later hydrothermal events. Multiple episodes of crack filling can involve any of the above mentioned minerals, as seen in Figure 7. This photomicrograph shows a plagioclase grain in a biotite monzogranite gneiss at a depth of 2634 m. The plagioclase grain has been fractured and sealed with more plagioclase that conforms to the twinning planes of the host grain. This crack filling was subsequently opened in tension and refilled with a zeolitic material. Note the close agreement between the two sides of the plagioclase filling, showing that the crack movement was dilitational, as would be expected during hydrofracturing of the rock. The examples discussed above

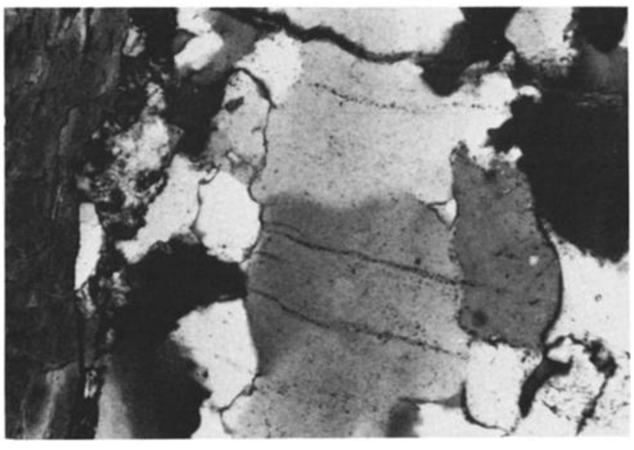

Fig. 5. Healed cracks in quartz. A string of fluid inclusions marks the former position of a fracture plane. 0.9-mm-wide image.

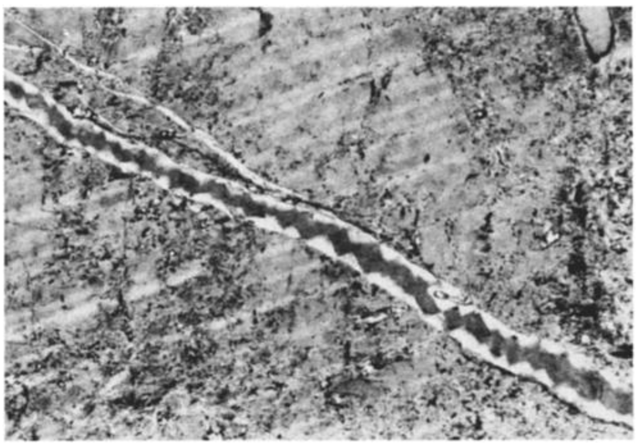

Fig. 7. Plagioclase grain in a biotite monzogranite gneiss at 2634 m. The grain was fractured and filled with plagioclase along the twinning planes. The vein was later reopened and filled with a zeolitic mineral. 0.9-mm-wide image.

all illustrate various hydrothermal processes that generally reduce the permeability of the rock.

DISCUSSION

One of the principle objectives of the DOSECC drill hole at Cajon Pass was to try and resolve the long-standing discrepancy between high heat flow predicted from faulting models and laboratory data on the one hand and the absence of a measurable heat flow anomaly across the San Andreas on the other. Rock permeability is important to this discussion because of the implications of fluid flow in and around fault zones. If we assume that the fault is strong with the associated high heat flow, then the frictionally generated heat must be removed by ground circulation in order to satisfy the constraints of the heat flow measurements. The regional permeability must be sufficiently high to accommodate the massive lateral movement of fluids in this case. This condition must be assessed both in terms of the intact permeability and the fracture permeability of the rocks. The intact permeability has been addressed in this paper, and we will begin the discussion with this topic.

The petrographic studies have shown that extensive crack healing and sealing have left few open pathways for fluid flow. The resulting permeability values are as low as 10^{-21} to 10^{-22} m^2, which is uncommon for other crystalline rocks studied under similar effective pressures. Typical permeabilities measured for surficially derived rocks such as Westerly, Barre or Chelmsford Granites are 2–3 orders of magnitude higher than the Cajon samples, in the range of 10^{-18} to 10^{-19} m^2 [*Brace et al.*, 1986]. These standard granites do not reach the low permeability values typical of the Cajon Pass rocks until crack closing pressures of a few hundred megapascals are applied. The difference between these results may have important implications for how we interpret permeabilities at depth. The permeability measurements on such rocks are generally made by loading a sample under increasingly higher pressures to simulate depth. The resulting permeability response is mechanical in nature (see for instance, *Walsh* [1981]). In contrast, the Cajon Pass rocks have been sampled from different sections within the drill hole, where they have been subject to variations in temperature, geochemical environment and degree of metamorphism [*Silver et al.*, 1989], in addition to the increasing lithostatic load. As a result, other processes may contribute to the permeability response (diffusion, hydrothermal alteration, etc.) which would not be observed in samples that are all derived from the same block of quarried rock. Therefore it may be unwise to make estimates of the permeability profile with depth based on such rocks. Similarly, it may be inappropriate to extrapolate the rapid decrease in permeability of the Cajon Pass samples to immeasurably low values at greater depth without a thorough understanding of the differences between the cored and surface samples.

The laboratory measurements give a lower limit to the bulk permeability in the region of the drill hole as they do not include large faults and joints that are present in situ. How do the measured values compare with the in situ environment? Unfortunately, there is limited in situ permeability data available to supplement the extensive laboratory data. Measurements made at a depth of 2000 m in the drill hole yield a bulk permeability of around 2×10^{-18} m^2 [*Coyle and Zoback*, 1988]. Although this value is a few orders of magnitude higher than the laboratory measurements, it is still quite low compared to typical in situ values compiled by *Brace* [1980]. By assuming that fluid flow is restricted to fractures observed on the borehole televiewer log, *Coyle and Zoback* [1988] calculate a fracture permeability ranging from 5 to 12×10^{-18} m^2. In light of the fact that the intact permeability is so low, the results suggest that fluid flow in the vicinity of the drill hole is probably limited to such fractured zones.

In the absence of more in situ values, what other evidence is there that the permeability around the San Andreas fault is low, even on a large scale? For this answer, we might look to some of the geochemical evidence. *Kharaka et al.* [1988, 1989] report on the fluid chemistry of water and associated gases collected from fracture systems at different test intervals in the lower part of the drill hole. Two of the test intervals, at 1829–1905 and 1829–2115 m, sampled fracture systems that were spatially close, with isotope values that indicate a meteoric origin of water. Fluid chemistries were markedly different in the two regions however, particularly the concentrations of Na, HCO_3, and SO_4. This suggests that these waters had undergone separate evolutionary paths and were isolated from one another in spite of the proximity of the fracture systems. If little mixing occurs even in the presence of fracture zones, it implies that the bulk of permeability of the rocks must be quite low.

Additional evidence of limited permeability comes from radon concentrations [*Hammond et al.*, 1988] and helium isotope studies [*Torgersen*, 1989]. Torgersen reports that isotopic compositions and helium concentrations of the formation waters at 2000 m vary between the fracture systems, indicating poor interconnection and limited mixing of fluids as observed by *Kahara et al.* [1988, 1989]. Pore fluid ages of 33,000 to 5×10^6 years were calculated from the ^4He data. Although this is quite a spread of age, even the youngest estimate would imply minimal heat transport by fluid flow, based on calculations of distance and time. These geochemical studies all support the notion that fluid flow and hence permeability must be extremely low, as we have measured in the laboratory, even though fracture systems intersect the drillhole in many regions.

How do these observations compare with the permeability necessary for massive water circulation? Models of convective heat transfer in the vicinity of the San Andreas give a minimum permeability value of 10^{-15} m^2 to account for the fricationally generated heat [*Coyle and Zoback*, 1989]. This is higher than any of the values that have been measured in the laboratory or in situ. The evidence presented here does not support the high stress hypothesis, as the low permeabilities can no accommodate the necessary massive water circulation. The permeability and geochemical observations are more consistent with the hypothesis of a weak fault based on the lack of a heat flow anomaly in the area. *Lachenbruch and Sass* [1989] have measured conductive heat flow at many depths in the Cajon Pass drill hole. Ironically, the shallow measurements were higher (90–100 mW/m^2) than the background levels of 70 mW/m^2 measured at other holes in the vicinity. These higher values can be explained by the rapid uplift and erosion of sediments in the area during Pleistocene times. Continued measurements to 3500 m show that the heat flow values drop off toward background levels as expected based on heat conduction models of such an erosional event. *Lachenbruch and Sass*

[1989] find no evidence that the measured heat flow has been affected by groundwater circulation, as required by the strong fault model. These findings imply that the average shear stresses acting on the fault are low, of the order of 10–20 MPa. Such values are consistent with the seismic stress drops of earthquakes [*Hanks*, 1977]. However, the weak fault model presents some problems which are not readily resolved when we try to reconcile the strength magnitude and orientation with the constitutive properties of the fault zone materials. If the principle stresses are nearly normal to the fault as suggested by *Zoback et al.* [1987], high fluid pressures would cause hydrofracturing of the rocks before the reduction in effective stress was sufficient to cause slip on the fault. Clearly, other mechanisms must be acting to reduce the coefficient of friction of the fault zone. Anomalously weak fault gouge material has been called upon to resolve this problem [*Zoback et al.*, 1987], although there is no conclusive evidence to confirm that such a gouge is responsible for the low stresses. *Radney and Byerlee* [1988] found that even montmorillonite, the lowest strength material likely to exist in fault zones, supports higher average shear stresses than the heat flow data would prescribe. Clearly, this controversy is by no means resolved. The factors that control the strength and constitutive properties must be better understood in order to explain the occurrence of earthquakes along the San Andreas fault.

SUMMARY OF RESULTS

1. Permeabilities of unfractured Cajon Pass core samples were very low, of the order of 10^{-19} to 10^{-22} m^2 measured at effective pressures corresponding to the depth of the samples. These values are 2–3 orders of magnitude lower than typical permeabilities reported in the literature for other granite rocks.

2. Repeated episodes of hydrothermal activity have sealed and healed the fractures, restricting fluid flow through the rock.

3. The low permeabilities argue against massive water circulation through the bulk of the rock as a mechanism for transporting frictionally generated heat away from the San Andreas fault. This is consistent with the geochemical evidence of little mixing of the pore waters from different regions of the drill hole.

Acknowledgment. This research was supported by the USGS under the Deep Continental Studies Program.

REFERENCES

Bear, J., *Dynamics of Fluids in Porous Media*, American Elsevier, New York, 1972.
Brace, W. F., Permeability of crystalline and argillaceous rocks, *Int. J. Rock Mech. Min. Sci. Geomech. Abstr.*, *17*, 241–251, 1980.
Brace, W. F., and D. L. Kohlstedt, Limits on lithospheric stress imposed by laboratory experiments, *J. Geophys. Res.*, *85*, 6248–6252, 1980.
Brace, W. F., J. B. Walsh, and W. T. Frangos, Permeability of granite under high pressure, *J. Geophys. Res.*, *73*, 2225–2236, 1968.
Coyle, B. J., and M. D. Zoback, In situ permeability and fluid pressure measurements at 2 km depth in the Cajon Pass research well, *Geophys. Res. Lett.*, *15*, 1027–1032, 1988.
Hammond, D. E., B. W. Leslie, T.-L. Ku, and T. Torgersen, ^{222}Rh concentrations in deep formation waters and the geohydrology of the Cajon Pass borehole, *Geophys. Res. Lett.*, *15*, 1045–1048, 1988.
Hanks, T. C., Earthquake stress drops, ambient tectonic stresses and stresses that drive plate motions, *Pure Appl. Geophys.*, *115*, 441–458, 1977.
Healy, J. H., and Zoback, M. D., Hydraulic fracturing in situ stress measurements to 2.1 km depth at Cajon Pass, California, *Geophys. Res. Lett.*, *15*, 1005–1008, 1989.
Kharaka, Y. K., L. D. White, G. Ambats, and A. F. White, Origin of subsurface water at Cajon Pass, California, *Geophys. Res. Lett.*, *15*, 1049–1052, 1988.
Kharaka, Y. K., G. Ambats, W. C. Evans, and L. D. White, Fluid chemistry in three test intervals at Cajon Pass, Eos, *Trans. AGU* *70*(15), 481, 1989.
Lachenbruch, A. H., and J. H. Sass, Heat flow and energetics of the San Andreas fault, *J. Geophys. Res.*, *85*, 6185–6222, 1980.
Lachenbruch, A. H., and J. H. Sass, Decreased heat flow with depth in the scientific research well at Cajon Pass, California: Implications, Eos *Trans. AGU* *70*(15), 481, 1989.
Morrow, C., and J. Byerlee, Permeability of rock samples from Cajon Pass, California, *Geophys. Res. Lett.*, *15*, 1033–1036, 1988.
Morrow, C. A., L. Q. Shi, and J. D. Byerlee, Permeability of fault gouge under confining pressure and shear stress, *J. Geophys. Res.*, *89*, 3193–3200, 1984.
O'Neil, J. R., and T. C. Hanks, Geochemical evidence for water-rock interaction along the San Andreas and Garlock faults of California, *J. Geophys. Res.*, *85*, 6286–6292, 1980.
Pezard, P. A., and S. M. Luthi, Borehole electrical images in basement of the Cajon Pass scientific drillhole, California: Fracture identification and tectonic implications, *Geophys. Res. Lett.*, *15*, 1017–1020, 1988.
Radney, B., and J. Byerlee, Laboratory studies of the shear strength of montmorillonite and illite under crustal conditions, *Eos Trans. AGU*, *69*(44), 1463, 1988.
Silver, L. T., and E. W. James, The Cajon Pass Scientific drillhole: Keyhole to southern California geologic evolution, *Eos Trans. AGU*, *70*(15), 481, 1989.
Silver, L. T., E. W. James, S. J. Cotkin, and B. Chappell, Preliminary lithologic column from leg two of Cajon Pass drilling, *Eos Trans. AGU*, *70*(15), 482, 1989.
Sun, Y., and C.-Y. Wang, Microfractures in oriented cores from Cajon Pass drilling project in S. California, and stress field near the San Andreas fault, *Eos Trans. AGU*, *70*(15), 481, 1989.
Torgersen, T., Helium accumulation in Cajon Pass pore fluids: Geochemical constraints on pore fluid ages, hydrothermal heat flux and mass transport mechanisms, *Eos Trans. AGU*, *70*(15), 481, 1989.
Walsh, J. B., Effect of pore pressure and confining pressure on fracture permeability, *Int. J. Rock Mech. Min. Sci. Geomech. Abstr.*, *18*, 424–435, 1981.
Zoback, M. D., and J. H. Healy, Overview of in situ stress measurements in the Cajon Pass drillhole to a depth of 3.5 km, *Eos Trans. AGU*, *70*(15), 480, 1989.
Zoback, M. D., et al., New evidence on the state of stress of the San Andreas fault system, *Science*, *238*, 1105–1112, 1987.

J. D. Byerlee and C. A. Morrow, U.S. Geological Survey, MS 977, 345 Middlefield Road, Menlo Park, CA 94025.

(Received September 1, 1989;
revised January 9, 1990;
accepted January 29, 1990.)